Colloid Polym Sci 275:876–882 (1997)
© Steinkopff Verlag 1997

ORIGINAL CONTRIBUTION

F. Berger
I. Dékány

Multilayer adsorption with variable thickness at solid–liquid interfaces

Received: 2 April 1997
Accepted: 10 June 1997

F. Berger · Prof. I. Dékány (✉)
Department of Colloid Chemistry
Attila József University
6720 Szeged, Hungary

Abstract The multilayer adsorption on the solid/liquid interface in binary mixtures was studied by adsorption space filling with constant and variable layer thickness. Adsorption from benzene/n-heptane mixtures was examined on hydrophilic and hydrophobic surfaces. The free enthalpy of adsorption, $\Delta_{21}G = f(x_1)$, was calculated from the adsorption excess isotherm by integration of the Gibbs equation. Supposing that the free enthalpy is mainly due to adsorption in the first layer, the composition of this layer can be calculated from the $\Delta_{21}G = f(x_1)$ function. It was established that the adsorption layer thickness in benzene/heptane mixtures increases significantly with increasing benzene content. This statement was supported by X-ray diffraction on hydrophobic clay minerals.

Key words Adsorption – multilayers – binary mixtures – layer thickness – surface layer composition – adsorption capacity – free enthalpy of adsorption

Introduction

The interpretation of the adsorption excess isotherms at solid–liquid interfaces raises the question whether the adsorption is restricted to a monolayer or forms multilayers and whether the thickness of the adsorption layer is dependent on the composition of the bulk phase. Results published in the literature are not uniform in this respect since both monolayer [1–3] and multilayer models [4–7] are employed in the calculations. In this paper we show that a monolayer or a multilayer with constant thickness are extreme cases and are strictly associated with the linear region of the excess isotherm [1–4, 8–12]. We present excess isotherms (in benzene–n-heptane mixtures) which are to a transition from a monolayer to a multilayer coverage on the solid surface. Our calculations are based on the so-called parallel layer model where intermolecular interactions are also taken into consideration for calculating the layer thickness. When adsorption excess isotherms exist without linear regions, it is postulated that realistic information about the adsorption equilibrium will only be obtained by applying the model to a variable adsorption layer thickness.

The appearance of multilayer adsorption needs to be proved by independent methods. The dependence of mono- or multilayer adsorption on composition is unambiguously proven by interlamellar adsorption between pillared or hydrophobic clay mineral silicate layers, where the basal spacing can be determined by X-ray diffraction [10–12].

Theoretical background

The adsorption space filling model

The "space filling" model is often used for describing the equilibrium between the adsorbed layer and the bulk phase [1–4, 13–17]. In this model the volume of the adsorption layer is

$$V^s = t^s a^s = n_1^s V_{m,1} + n_2^s V_{m,2} = n_{1,0}^s V_{m,1}\ , \tag{1}$$

where t^s is the thickness of the adsorption layer, a^s the specific surface area of the adsorbent, n_i^s the amount of the ith component in the surface layer, $V_{m,i}$ is the partial molar volume of this component in the surface layer (in praxis the molar volume of the pure component i is used) and $n_{1,0}^s$ is the adsorption capacity related to the pure component 1.

The solid/liquid interfacial adsorption is characterized by the reduced adsorption excess amount according to the Ostwald–Izaguirre equation [2–4]:

$$n_1^{\sigma(n)} = n_1^s - n^s x_1 = n^s(x_1^s - x_1) \tag{2}$$

where n^s is the material content of the surface phase and $n^s = n_1^s + n_2^s$. If the excess amount $n_1^{\sigma(n)}$ is determined experimentally and the adsorption volume V^s (from $n_{1,0}^s$ or $n^s = n_1^s + n_2^s$) is known, the surface layer composition x_1^s can be calculated as follows:

$$x_1^s = \frac{r n_1^{\sigma(n)} + x_1 V^s/V_{m,1}}{V^s/V_{m,1} + n_1^{\sigma(n)}(r-1)}\ , \tag{3}$$

where r is the ratio of molar volumes, $r = V_{m,2}/V_{m,1}$. The so-called Everett–Schay equation is also often used [2, 3, 13, 15, 16]:

$$\frac{x_1 x_2}{n_1^{\sigma(n)}} = \frac{1}{n_{1,0}^s}\left[\frac{r}{S-1} + \frac{S-r}{S-1}x_1\right]\ , \tag{4}$$

where S is the separation factor of adsorption ($S = x_1^s x_2 / x_2^s x_1$). The value of S varies with the adsorption equilibrium constant $K = [(x_1^s)^r x_2]/[(x_1)^r x_2^s]$, neglecting the corresponding activity coefficients in the bulk and interfacial phases, if $r \simeq 1$.

When S is independent of x_1, the $x_1 x_2 / n_1^{\sigma(n)}$ vs. x_1 plot is linear [2, 3]. The values of $n_{1,0}^s$ and S are calculated from the slope and intercept, and $V^s = n_{1,0}^s V_{m,1}$.

If the layer thickness t^s e.g. $V^s = t^s a^s$ is also constant, the adsorption excess can be calculated from Eq. (3):

$$n_1^{\sigma(n)} = \frac{t^s a^s}{x_1^s V_{m,1} + (1 - x_1^s)V_{m,2}}(x_1^s - x_1)\ . \tag{5}$$

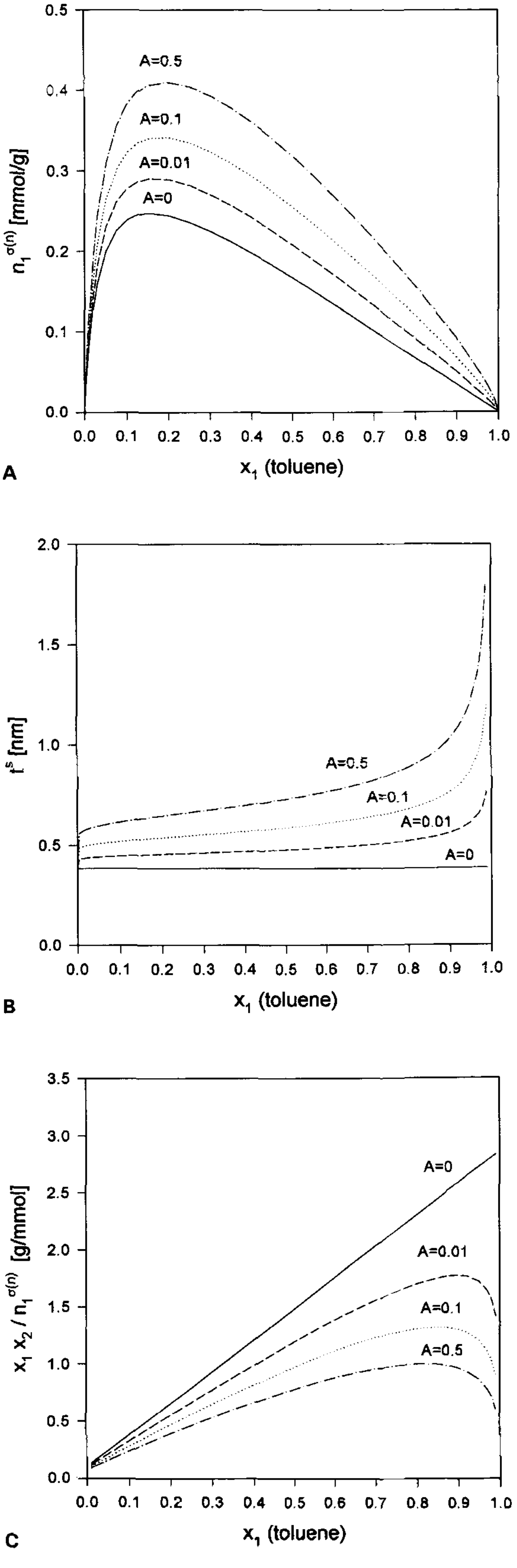

Fig. 1A Calculated adsorption excess isotherms in toluene (1)-cyclohexane (2) on solids with different A values of the FHH equation, $K = 30$, $B = 3$ (K is the equilibrium constant: $K = [(x_1^s)^r x_2]/[(x_1)^r x_2^s]$; **B** The adsorption layer thickness in toluene (1)-cyclohexane (2) on solids with different A values of the FHH equation, $K = 30$, $B = 3$; **C** The Everett–Schay representation of the excess isotherms. Notation as in Fig. 1A

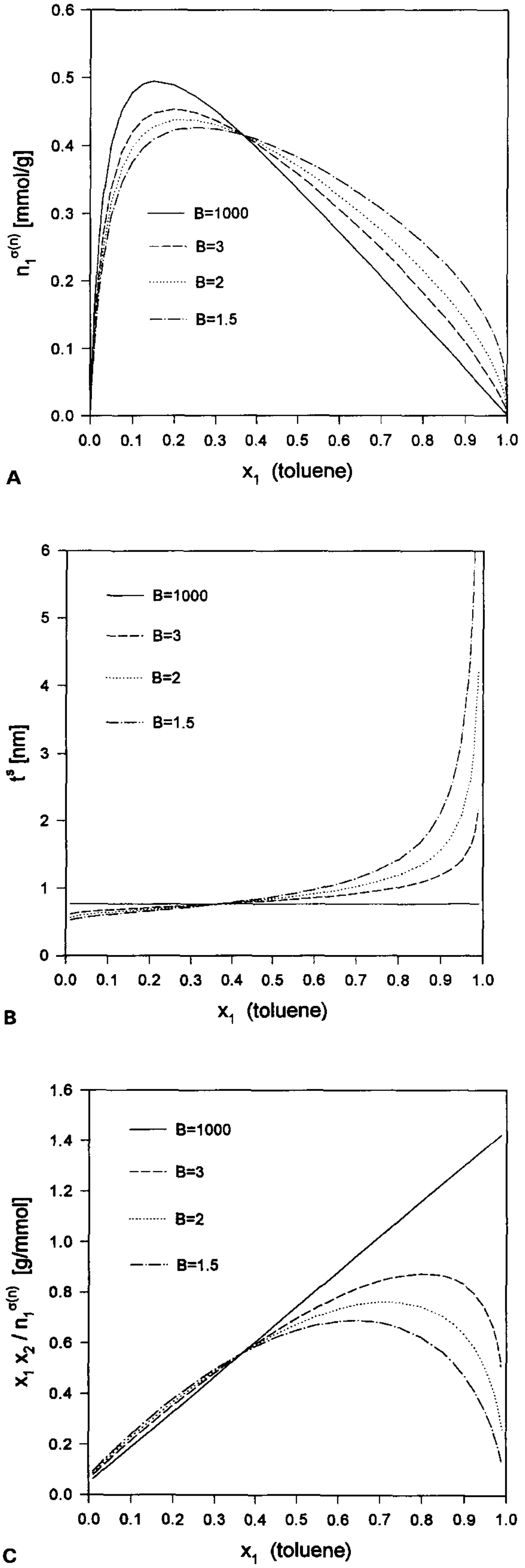

Fig. 2A Calculated adsorption excess isotherms in toluene (1)-cyclohexane (2) mixtures on solids with different B values of the FHH equation, $K = 30$, $A = 1$; **B** The adsorption layer thickness in toluene (1)-cyclohexane (2) on solid with different B values of the FHH equation, $K = 30$, Al = 1; **C** The Everett-Schay representation of the excess isotherms. Notation as in Fig. 2A

Of course, t^s need not be constant, but can be a function of the bulk phase composition.

We return to the examination of the toluene–cyclohexane series assuming that the thickness of the adsorption layer is no longer constant but changes according to the Frenkel–Halsey–Hill isotherm [18]:

$$t^s = 0.384\ \mathrm{nm}\ [1 + (A/\ln(1/x_1))^{1/B}]\ , \tag{6}$$

where B is related to the rate of fall-off of the adsorption potential with distance from the surface and A is an intermolecular interaction constant. The layer thickness is a function of the composition x_1, shown in Fig. 1A and 1B for different values of A.

If the parameter B is varied and the value of A is kept constant ($A = 1$), a series of isotherms is obtained which intersect at $x_1 = 0.37$ (Fig. 2). The isotherm corresponding to $B = 1000$ has a linear region at $x_1 = 0.2$–1.0, i.e. Schay–Nagy extrapolation can be used for determining adsorption capacity [2–4]. When B decreases, the isotherms are inclined (Fig. 2A), because the adsorption layer becomes thicker than monomolecular. Model computations reveal a significant increase in the number of layers especially in the range of $x_1 \geq 0.6$. The isotherms exhibit a curvature and the plot $x_1x_2/n_1^{\sigma(n)} = f(x_1)$ will also be nonlinear (Fig. 2C).

The model calculations described above prove that only in the case of constant layer thickness or monomolecular coverage, at $r \simeq 1$ and $K = 10^3$–10^2 (i.e. under conditions of preferential adsorption), both the Schay–Nagy extrapolation and the Everett–Schay function are suitable for the determination of the adsorption capacity of the pure component $n_{1,0}^s$.

Calculation of the equivalent layer thickness: $t^s_{equ} = f(x_1)$

The strategy of our calculations is based on the assumptions: (1) the adsorption layer is made up of parallel monolayers, (ii) surfacial enrichment decreases nearly exponentially, (iii) the free enthalpy of displacement, $\Delta_{21}G$ is mainly related to adsorption of the first layer (Fig. 3):

$$\Delta_{21}G = \sum_{i=1}^{\infty} \Delta_{21}G_i\ , \tag{7}$$

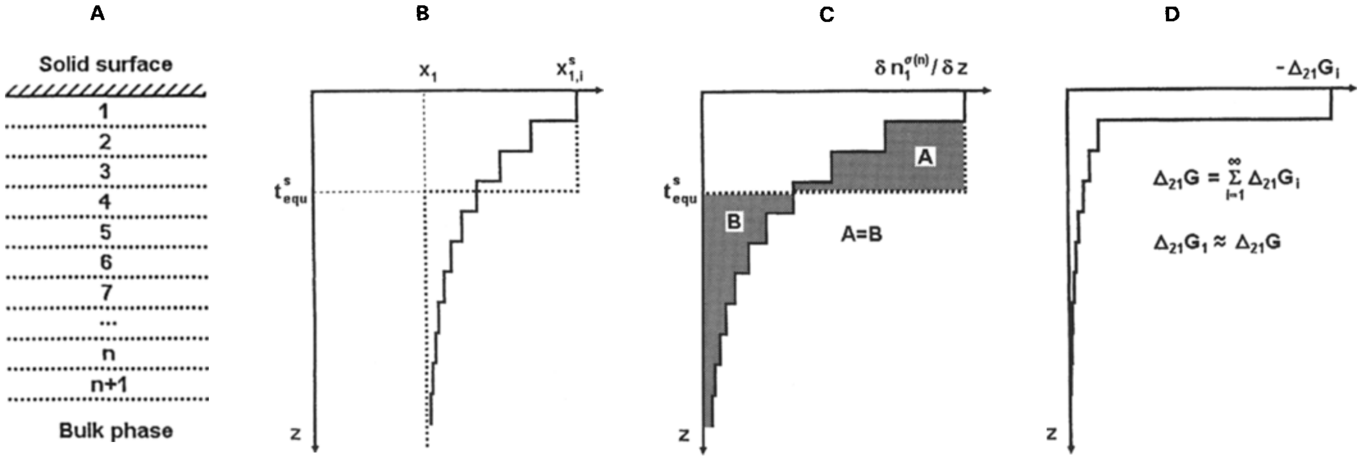

Fig. 3 Schematic structure of the solid/liquid interfacial layer: **A** solid/liquid interface with multilayers; **B** surface layer composition (x_i^s) as a function of the distance (z) from the surface, x_1: the equilibrium bulk composition, t^s_{equ}: equivalent layer thickness: **C** excess density function against the distance: the area of A is equivalent with the area of B. The total area under the density function $\delta n_1^{\sigma(n)}/\delta z$ is the surface excess amount; **D** the free enthalpy distribution function from the surface.

where $\Delta_{21}G_i$ is the free enthalpy of the displacement in the ith monolayer.

In order to characterize the layer thickness in the case of a diffuse adsorption layer, we propose the use of the "equivalent layer thickness" t^s_{equ}. It represents the thickness of a homogeneous surface layer which has the same composition as the first monolayer (i.e. $x_1^s = x_{1,1}^s$) and contains *equivalent* excess amount, i.e., $A = B$ at t^s_{equ} distance (see Fig. 3B and 3C).

The function $\Delta_{21}G$ vs. x_1 is obtained by integrating the Gibbs equation [1–7, 19]:

$$\Delta_{21}G = -RT \int_{a_1^*=0}^{a_1} \frac{n_1^{\sigma(n)}}{x_2 a_1^*} \, da_1^* , \tag{8}$$

where a_1 is the activity of component 1 in the bulk phase and $a_1 = \gamma_1 x_1$. Activity coefficients for the benzene (1)/ n-heptane (2) mixtures were calculated by the Redlich–Kister 5-parameter equation using the vapour–liquid equilibrium data [20, 21].

Several equations are suitable for calculation of $\Delta_{21}G$ for the parallel layer model. After some comparative tests we concluded that the following equation yields the best results [15, 16]:

$$\Delta_{21}G_1 = RT \frac{a^s}{a_{m,1}} \left[\frac{1}{r} \ln \frac{\Phi_2^s}{\Phi_2} + \frac{r-1}{r} (\Phi_2^s - \Phi_2) \right] , \tag{9}$$

where Φ_2 is the volume fraction of component 2 in the bulk phase and $\Phi_2 = r(1 - x_1)/(x_1 + r(1 - x_1))$, Φ_2^s is the volume fraction of component 2 in the first monolayer, $\Delta_{21}G_1$ is the free enthalpy of displacement in the first monolayer, and $a_{m,1}$ is the molar cross-sectional area of component 1. When the values of Φ_2 and $\Delta_{21}G_1$ are known, Φ_2^s is calculated from Eq. (9).

Equation (9) has no analytical solution, but can be easily solved by iteration. It is advisable to write Eq. (9) in the following form.

$$\frac{-\Delta_{21}G_1 a_{m,1}}{RT a^s} + \frac{1}{r} \ln \frac{\Phi_2^s}{\Phi_2} + \frac{r-1}{r} (\Phi_2^s - \Phi_2) = 0 . \tag{10}$$

In this case we have a zero-place determination problem which can be solved with one of the common methods (e.g. interval-halving method, secant-method, Newton–Raphson method, etc.).

After the determination of Φ_2^s the composition $x_{1,1}^s$ in the first monolayer can be calculated as follows:

$$x_{1,1}^s = \frac{r(1 - \Phi_2^s)}{\Phi_2^s + r(1 - \Phi_2^s)} \tag{11}$$

According to Eqs. (9) and (11) the equivalent layer thickness is

$$t^s_{equ} = \frac{n_1^{\sigma(n)} V_{m,1}}{a^s} \frac{x_{1,1}^s + r(1 - x_{1,1}^s)}{x_{1,1}^s - x_1} . \tag{12}$$

Materials and methods

Materials

Benzene and n-heptane of analytical purity were dried over Linde 4A molecular sieve. Three different adsorbents were used: the hydrophobized silica R972, $a^s_{\mathrm{BET}} = 115\,\mathrm{m^2/g}$ (Degussa AG, Germany), a pillared Na-mont morillonite, $a^s_{\mathrm{BET}} = 132.8\,\mathrm{m^2/g}$, and dodecylammonium-vermculite.

The Al-pillared montmorillonite (Al-PILC) was prepared from Na-montmorillonite with polyhydroxoaluminium ions. In the polyhydroxoaluminium solution Al concentration was 0.1 M, the OH/Al ratio was 2:1, the Al montmorillonite concentration 6.8 mmol $\mathrm{g^{-1}}$.

The dodecylammonium-vermiculite was prepared from vermiculite (South Africa, cation exchange capacity (CEC): 1.97 mmol $\mathrm{g^{-1}}$, specific surface area from crystal geometry: 788 $\mathrm{m^2\,g^{-1}}$) by cation exchange with dodecylammonium chloride solution (0.1 M surfactant in 1.4-fold excess related to CEC, pH = 4.5). The organo derivative was washed several times with alcohol–water mixtures = 1:1 for 48 h and dried in vacuum oven at 333 K.

Methods

The excess isotherms ($n_1^{\sigma(n)} = f(x_1)$) were determined at 298 ± 0.5 K [2–4]. The composition of the liquid mixtures before and after adsorption was measured with a liquid interferometer (Zeiss, Jena) [8–12].

The basal spacing, d_L of dodecylammonium vermiculite in benzene-n-heptane mixtures were measured by an X-ray powder diffractometer (Philips PW 1820/PW 1830) [10–12].

Results

Figure 4 shows the excess isotherm for benzene (1)/n-heptane (2) mixtures on Al-PILC and the calculated equivalent layer thickness. As the basal spacing determined by X-ray diffraction is 1.78 nm and the thickness of the silicate layer is 0.96 nm, 0.82 nm is the thickness of the interlamellar space, i.e. 0.41 nm per surface. If, based on the data published in the literature [8–12], the cross sectional area of one benzene molecule is 0.38 $\mathrm{nm^2}$ [22], 0.41 nm corresponds to 1.05 molecular layers, i.e., a monomolecular adsorption layer. This is in excellent agreement with the value predicted by the model.

Figure 5 presents the excess isotherm determined on hydrophobized silica R972 and the changes in the specific layer thickness as a function of x_1. The minimal layer thickness and minimal layer number necessary for a thermodynamically consistent description of adsorption is calculated for each excess isotherm on the basis of the so-called Rusanov criterion [2–4]. In the present case the value of this minimal layer number at low values of x_1 is about 1 or even lower while at high values of x_1 it is about 3. The equivalent layer thickness calculated for the parallel layer model satisfies this criterion.

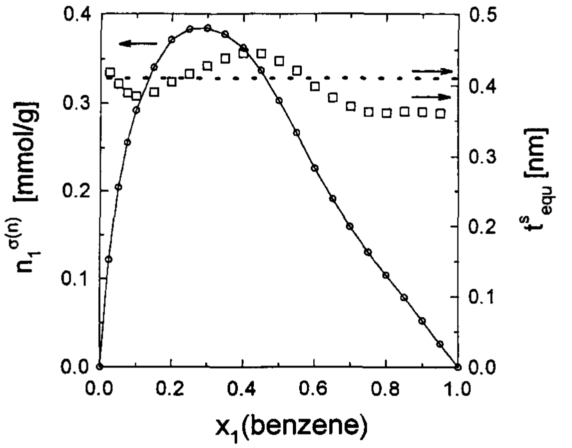

Fig. 4 Adsorption excess isotherm on pillared montmorillonite in benzene-(1)-n-heptane (2) and equivalent layer thickness function calculated by Eq. (12)

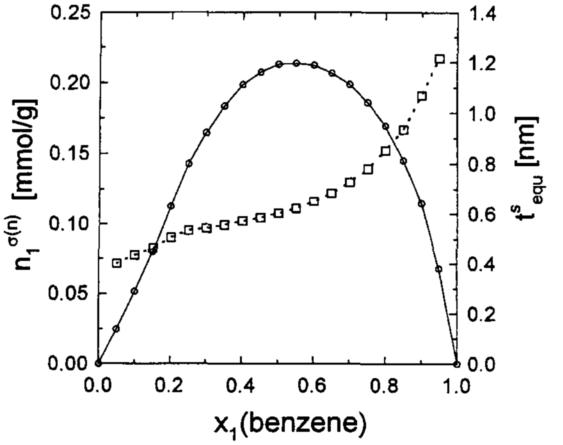

Fig. 5 Adsorption excess isotherm on aerosil R972 in benzene-(1)-n-heptane (2) and equivalent layer thickness calculated by Eq. (12)

The behaviour of dodecylammonium vermiculite was studied in benzene/n-heptane mixtures. Figure 6 shows the excess isotherm and basal spacings. For the benzene content of $x_1 = 0.5$–0.7 the layers move apart, and the adsorption excess increases steeply. This process may be divided into two steps (Figs. 7 and 8). Adsorption in step 1 occurs only on the external surface, at $x_1 < 0.4$. Process $1 \rightarrow 2$ begins with adsorption on the external surface; however, adsorption on the internal surfaces of the interlamellar space dominates at $x_1 > 0.7$. Changes in the interlamellar structure of C_{12}-vermiculite at different adsorption equilibrium compositions clearly support this view (Fig. 7). Assuming an angle of $\alpha = 55°$ between the alkyl chains and

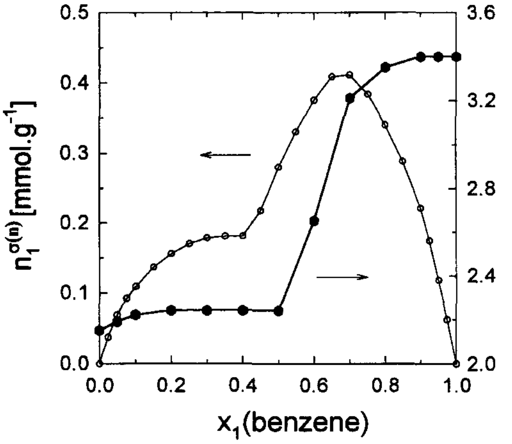

Fig. 6 Adsorption excess isotherm and basal spacing of dodecylammonium vermiculite in benzene-(1)-n-heptane (2)

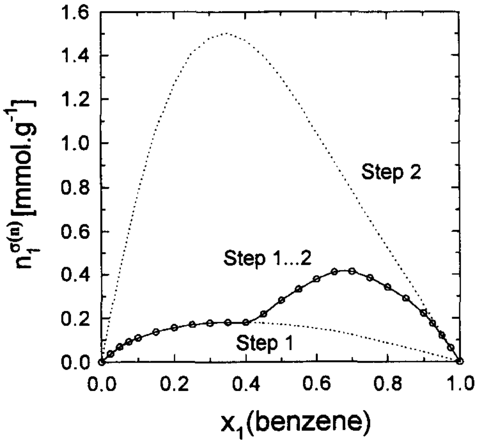

Fig. 8 Adsorption excess isotherm and calculated isotherms in benzene-(1)-n-heptane (2)

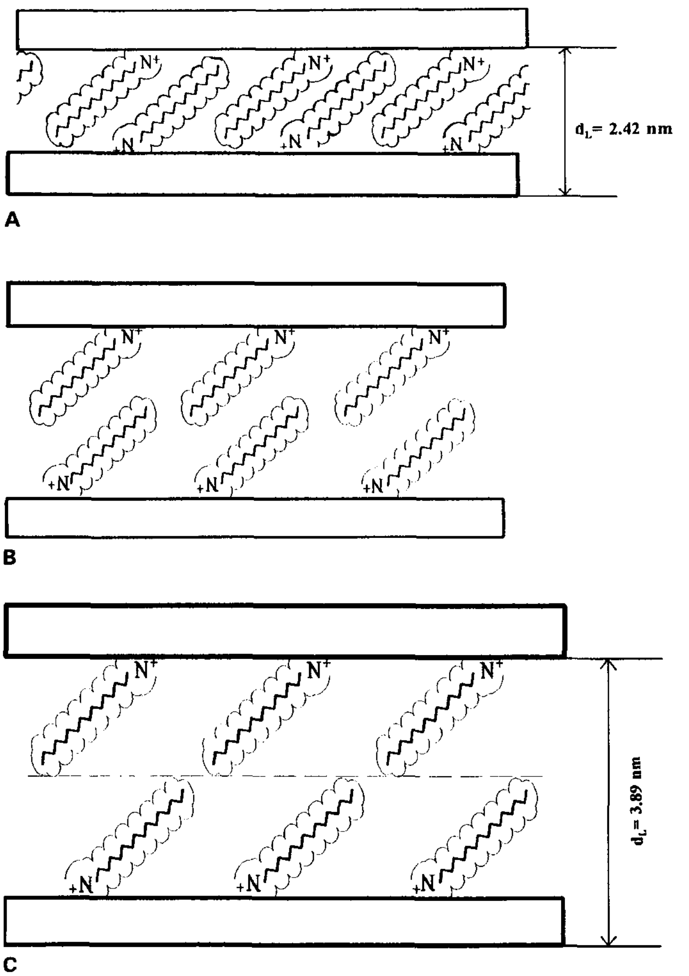

Fig. 7 Model of alkyl chain orientation (tilting angle $\alpha = 55°$) with increasing concentration of benzene (2); **A.** Monolayer structure in n-heptane (1), **B.** Swelling at $x_1 = 0.5–0.6$, **C.** bilayer structure at maximum swelling

the silicate surface, three different stages of swelling may be distinguished [11, 12]. Figure 7A describes the non-expanded state when in n-heptane and in mixtures rich in n-heptane adsorption occurs mostly on the external surfaces: $d_L = (12 \times 0.127 + 0.28) \sin 55° + 0.94 = 2.42$ nm (step 1). The transition state (Fig. 7B) is followed by full interlamellar expansion (Fig. 7C), when the alkyl chains still touch each other. The experimental data show that total expansion ($d_L = 3.89$ nm) is never realized in mixtures rich in benzene, since the experimentally determined value of d_L in pure benzene is only 3.40 nm. Step 2 and the corresponding hypothetical isotherm refer to a basal spacing of $d_L = 3.4$ nm calculated from the value of d_L and the silicate layer dimensions (Fig. 8). This result gives an excellent opportunity to compare the measured layer thickness and that calculated by Eqs. (9) and (12).

In addition to the isotherm $n_1^{\sigma(n)} = f(x_1)$, the value of specific surface area is also necessary for these calculations. Considering the unit cell dimensions and the content of organic matter, in step 2 the total surface area is 598 m^2 g^{-1}. Based on the ratio of $n_{1,0}^s$ adsorption capacities in steps 1 and 2 – calculated by Schay–Nagy extrapolation method – the estimated external surface is 60 m^2 g^{-1}.

Equivalent layer thickness functions calculated by Eqs. (9) and (12) for steps 1 and 1–2 using the above data, and also layer thicknesses calculated from XRD data are shown in Fig. 9. The equivalent layer thickness function of steps 1–2 changes in a similar way as the XRD layer thickness values. The relative deviation is not larger than 10% which may be regarded as a good agreement. When the equivalent layer thickness functions corresponding to steps 1 and 1–2 are compared to the t^s function obtained for R-972 (see Fig. 5), the difference between the behavior

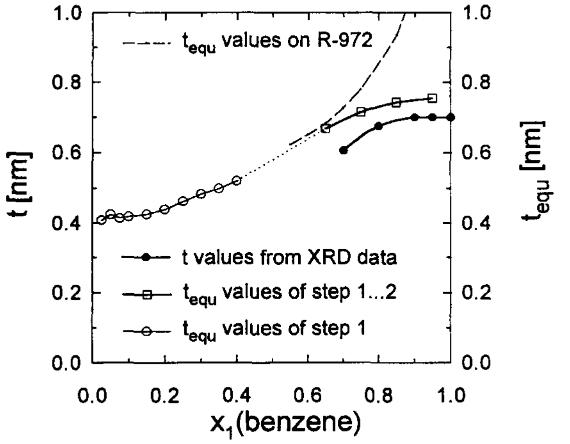

Fig. 9 The adsorption layer thickness in benzene-(1)-n-heptane (2) on dodecylammonium vermiculite and aerosil R972

of the adsorbent under conditions of unlimited expansion of the adsorption volume (R-972) and that of the adsorbent with limited swelling is quite evident.

Conclusion

If it is assumed that the layer thickness changes with composition [i.e. $t^s = f(x_1)$], the calculated excess isotherms exhibit a strong inclination. The extent of inclination indicates how much the thickness of the adsorption layer depends upon the composition of the bulk phase. The correctness of the method was checked on a pillared montmorillonite as adsorbent where the existence of adsorption monolayer is confirmed by X-ray diffraction.

Adsorption isotherms measured on dodecylammonium vermiculite in benzene/n-heptane describe adsorption on the external and interlamellar surfaces. The calculated thickness of the adsorption layer is verified by XRD measurements. The applicability of Eqs. (9) and (12) for calculating the adsorption layer thickness is acceptable within the limits of experimental error (±10%).

Acknowledgment The authors are very grateful to the Hungarian Research Scientific Fund, OTKA I/5 T007531, OTKA I/6 T014159 and to the Hungarian Ministry of Education MKM Pr. No. 219/1995.

References

1. Schay G, Nagy LG (1960) Periodica Polytechn 4:45
2. Schay G (1969) In Matijevic E (ed) Surface and Colloid Science, Vol 2. Wiley, London
3. Schay G (1969) In: Everett DH (ed) Surface Area Determination. Proc Int Symp, Butterworths, London
4. Kipling JJ (1965) Adsorption from Solutions of Non-Electrolytes. Academic Press, London
5. Tóth J (1970) Acta Chem Acad Sci Hung 63:67
6. Tóth J (1974) J Colloid Interface Sci 46:38
7. Marinin DV, Golikov AP, Viot AV, Avramenko VA and Gloshchenko VYu (1992) J Colloid Interface Sci 152:161
8. Dékány I, Szántó F, Nagy LG, Schay G (1983) J Colloid Interface Sci 93:151
9. Dékány I, Nagy LG, Schay G (1978) J Colloid Interface Sci 66:197–200
10. Dékány I, Szántó F, Weiss A, Nagy LG (1985) Ber Bunsenges Phys Chem 89:62–67
11. Dékány I, Szántó F, Weiss A, Lagaly G (1986) Ber Bunsenges Phys Chem 90:422–427
12. Dékány I, Szántó F, Weiss A, Lagaly G (1986) Ber Bunsenges Phys Chem 90:427–431
13. Everett DH (1964) Trans Faraday Soc 60:1803; (1965) 61:2478
14. Billett DH, Everett DH, Wright EEH (1964) Proc Chem Soc 216
15. Everett DH (1981) Pure Appl Chem 53:2181
16. Everett DH (1979) Colloid Science Vol 3, p 66. Chemical Society, London
17. Everett DH (1967) Progr Colloid Polym Sci 65:103
18. Halsey G (1948) J Chem Phys 16(10):931
19. Schay G (1976) Pure Appl Chem 48:393–400
20. Redlich O, Kister AT (1948) Ind Eng Chem 40:341
21. Scatchard G, Ticknor LB (1952) J Am Chem Soc 74:3724
22. McClellan AL, Harnsberger HF (1967) J Colloid Interface Sci 23:577
23. Dabrowski A, Jaroniec M (1980) J Colloid Interface Sci 7:571
24. Dabrowski A (1983) Monatscefte f Chemie 114:875
25. Dabrowski A (1986) Monatshefte f Chemie 117:139
26. Prigogine O, Maréchal J (1952) J Colloid Sci 7:122
27. Sardéa-Marhot L (1954) Bull Ac Poly Belg 40:1120
28. Findenegg GH (1971) J Colloid Interface Sci 35:249
29. Everett DH, Findenegg GH (1969) Nature 223:52
30. Findenegg GH (1973) J Chem Soc Faraday Trans 1, 69:1069
31. Rudzinski W, Partyka S (1981) J Chem Soc Faraday Trans 1, 77:2577
32. Rudzinski SW, Zajac J, Dékány I, Szántó F (1986) J Colloid Interface Sci 112:473